Neural Stem Cell-based Cell Carriers Enhance Therapeutic Efficacy of an Oncolytic Adenovirus in an Orthotopic Mouse Model of Human Glioblastoma

Atique U Ahmed[1], Bart Thaci[1], Nikita G Alexiades[1], Yu Han[1], Shuo Qian[1], Feifei Liu[1], Irina V Balyasnikova[1], Ilya Y Ulasov[1], Karen S Aboody[2] and Maciej S Lesniak[1]

[1]The Brain Tumor Center, The University of Chicago, Chicago, Illinois, USA; [2]Department of Neurosciences, City of Hope National Medical Center and Beckman Research Institute, Duarte, California, USA

The potential utility of oncolytic adenoviruses as anticancer agents is significantly hampered by the inability of the currently available viral vectors to effectively target micrometastatic tumor burden. Neural stem cells (NSCs) have the ability to function as cell carriers for targeted delivery of an oncolytic adenovirus because of their inherent tumor-tropic migratory ability. We have previously reported that *in vivo* delivery of CRAd-S-pk7, a glioma-restricted oncolytic adenovirus, can enhance the survival of animals with experimental glioma. In this study, we show that intratumoral delivery of NSCs loaded with the CRAD-S-pk7 in an orthotopic xenograft model of human glioma is able to not only inhibit tumor growth but more importantly to increase median survival by ~50% versus animals treated with CRAd-S-pk7 alone ($P = 0.0007$). We also report that oncolytic virus infection upregulates different chemoattractant receptors and significantly enhances migratory capacity of NSCs both *in vitro* and *in vivo*. Our data further suggest that NSC-based carriers have the potential to improve the clinical efficacy of antiglioma virotherapy by not only protecting therapeutic virus from the host immune system, but also amplifying the therapeutic payload selectively at tumor sites.

Received 16 September 2010; accepted 22 April 2011; published online 31 May 2011. doi:10.1038/mt.2011.100

INTRODUCTION

Glioblastoma multiforme remains one of the deadliest classes of human cancer with a median survival rate of ~15 months.[1] The standard-of-care therapy for newly diagnosed glioblastoma multiforme includes surgical resection, radiotherapy, and chemotherapy.[1] The success of these current therapies is, however, limited, because of the disseminated nature of these tumors. Consequently, there is a substantial need for the development of novel, effective, and less-toxic approaches to cancer therapy in order to improve patients' quality-of-life and increase their survival.

Oncolytic virotherapy for cancer is a novel approach where viruses are modified to preferentially replicate in tumor cells and selectively destroy them. During the past two decades a number of promising oncolytic viruses have demonstrated antiglioma activity in both preclinical and clinical settings.[2] However, the host's immune system imposes a significant challenge to the development of effective oncolytic viral therapy against human cancers. The majority of therapeutic virus delivered to a tumor site does not exist as free floating particles for longer than a few minutes at most,[3] which inhibits their ability to infect satellite tumor sites and thus limits antitumor efficacy.

Neural stem cells (NSCs) have recently received a great deal of attention because of their therapeutic potential for neurological disorders. In the last decade, many *in vitro* and *in vivo* studies have demonstrated that NSCs have the unique, inherent property to migrate throughout the brain and target invasive solid tumors, including gliomas.[4,5] This provides a novel platform for targeted delivery of anticancer agents selectively to disseminated tumors. In animal models, NSCs engineered to express a variety of therapeutic genes have been shown to migrate to distant tumor sites and selectively destroy neuroblastoma.[6,7]

Early *in vivo* experiments with oncolytic viruses revealed that infected virus-producing cells could also generate sustained antitumor activity when administered in place of therapeutic virus.[8] This led to the hypothesis that producer cells can be used to hide a therapeutic virus from the host immune system and when delivered systemically, travel to disseminated tumor burdens far from the injection site. Our lab recently reported a proof-of-concept study showing that NSCs can be used as a cell carrier to deliver CRAd-S-pk7, an oncolytic adenovirus, to intracranial glioma.[9] In this study, we expand upon this investigation to determine the optimal *ex vivo* conditions to load/infect oncolytic adenovirus into NSCs for *in vivo* delivery in an orthotopic human malignant glioma model in order to achieve clinically relevant therapeutic efficacy.

To achieve optimal delivery and therapeutic efficacy *in vivo*, cell carriers such as NSCs need to be loaded with the maximum dose of oncolytic virus that does not negatively affect carrier cell

Correspondence: *Maciej S Lesniak, The Brain Tumor Center, The University of Chicago, 5841 South Maryland Avenue, MC 3026, Chicago, Illinois 60637, USA. E-mail: mlesniak@surgery.bsd.uchicago.edu*

survival and tumor-homing property. To act as a Trojan horse and successfully hide the oncolytic virus from the host immune system, the cell carriers should ideally reach the tumor site before the viral progeny is released.[10] This study was specifically designed to identify and optimize such important parameters in the preclinical setting. Results presented in this study suggest that *in vivo* delivery of an oncolytic adenovirus by NSCs significantly reduced vector-induced neuroinflammation, thus sustaining a high vector titer intratumorally as compared with virus injected alone. Furthermore, we also examined the effects of oncolytic adenovirus loading on the tumor-tropic migratory property of NSCs and show for the first time that loading adenovirus into NSCs enhances their migratory ability. Finally, CRAd-S-pk7 oncolytic virus–loaded NSCs administered intracranially in an orthotopic glioma model significantly improved median survival. Thus, evidence presented in this study strongly argues in favor of the use of NSCs as a cell carrier for oncolytic virotherapy and suggests that such system may provide a viable strategy for tracking down and delivering a therapeutic payload to disseminated tumor burdens.

RESULTS

Cytopathic effects of CRAd-S-pk7 infection on NSCs and human glioma cell lines

We first examined the effect of CRAd-S-pk7 virus infection on the viability of NSCs and a panel of human glioma cell lines by using the trypan blue exclusion method at 96 hours postinfection. At low dose [0.1–1.0 infectious unit (I.U.)], we observed minimal toxicity induced by CRAd-S-pk7 virus in the NSCs compared to an untreated control (**Figure 1a**). On the other hand, U251 and the A172 glioma lines showed susceptibility to the cytopathic effects of CRAd-S-pk7 virus with approximately a 50% decrease in cell viability at these doses. When cells were infected with higher doses (10, 50, and 100 I.U.) of CRAd-S-pk7, both the NSCs and the glioma cell lines were susceptible to CRAd-S-pk7-induced lysis. However, NSCs were more resistant to CRAd-S-pk7-induced cytolysis as compared to all of the human glioma cell lines tested (when infected at a dose of 10 I.U., 70% of NSCs were viable as compared to average 30% of glioma cells, $^{**}P < 0.005$).

Replication kinetics of CRAd-S-pk7 virus in NSCs

In order to establish optimal conditions for *in vivo* delivery, we next studied the replication kinetics of the CRAd-S-pk7 virus in the carrier cells at the loading dose of 10 I.U. The extent of viral DNA replication was determined by measuring the number of viral E1A copies per ng of DNA from the infected cells by quantitative PCR. Viral DNA replication reached maximum levels at 48 hours postinfection (**Figure 1b**) followed by intracellular virus production, which reached its peak at 3 days postinfection (**Figure 1c**, **Supplementary Figure S1**). At 4 days postinfection,

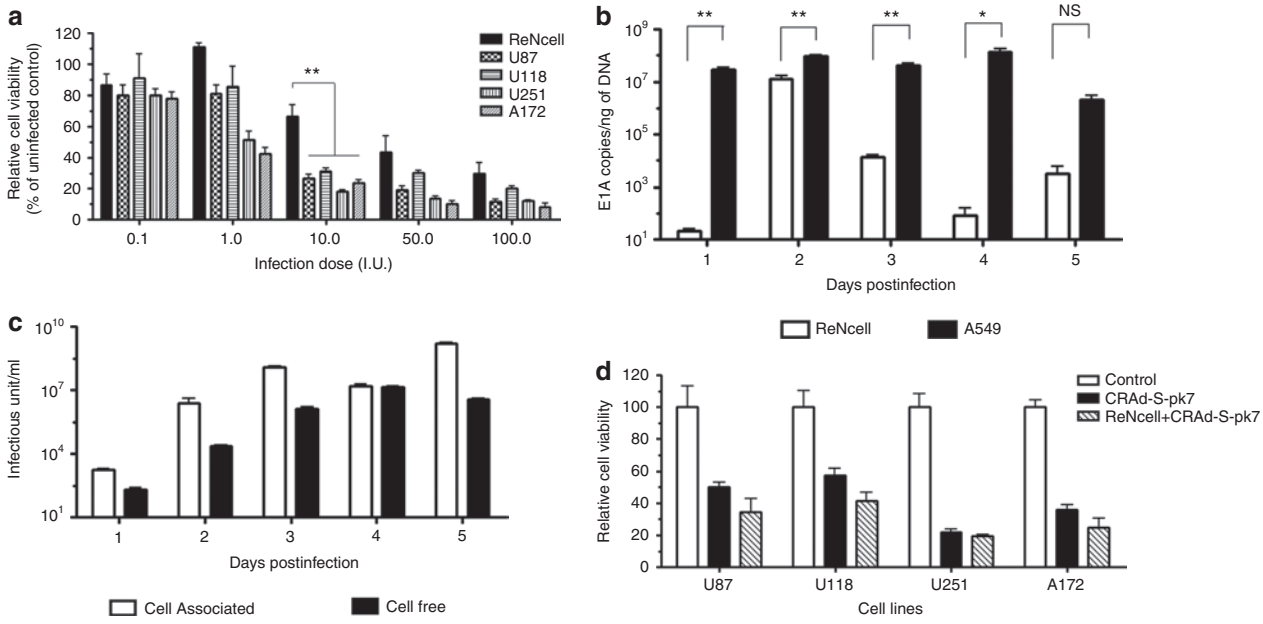

Figure 1 CRAd-S-pk7 efficiently replicates in neural stem cells. (**a**) Cytopathic effects of oncolytic adenovirus on neural stem cells (NSCs) and a panel of human glioma cell lines. Cells were infected with different I.U. of CRAd-S-pk7 and cell viability was evaluated by trypan blue exclusion method at 48 hours postinfection. All conditions were conducted in triplicate and repeated in three separate experiments (error bars represent SD). All the glioma cell lines tested were highly susceptible to CRAd-S-pk7 virus killing, whereas NSCs were less susceptible ($^{**}P < 0.005$ with 10 I.U. infection dose). (**b**) The replicative capacity of CRAd-S-pk7 was measured by quantitative RT-PCR. The extent of viral replication was determined by measuring the number of viral E1A copies per ng of DNA from the infected cells (error bars are SD). (**c**) Media and the cell plates were separated from the infected well. The total viral progeny in the cell plate (cell associated) and the progeny released by the infected NSCs (cell free) over time were measured by the titer assay. (**d**) Cytopathic effects of CRAd-S-pk7 virus released from loaded NSCs in a panel of human glioma cell lines. NSCs were loaded with the CRAd-S-pk7 virus at 50 I.U./cell for 2 hours and then washed and plated in the upper well of a transwell plate (5×10^3 cells/well). Equal amounts of naked CRAd-S-pk7 (2.5×10^5 I.U.) were also placed in the upper well. Four human glioma cell lines were placed in the bottom wells (5×10^4 cells/well) and incubated for 6 days, after which cell viability was evaluated by trypan blue exclusion method. CRAd-S-pk7 virus released from the loaded NSCs was able to kill the glioma cells in the bottom wells as efficiently as the naked virus. All conditions were conducted in triplicate and repeated in two separate experiments (error bars are SD).

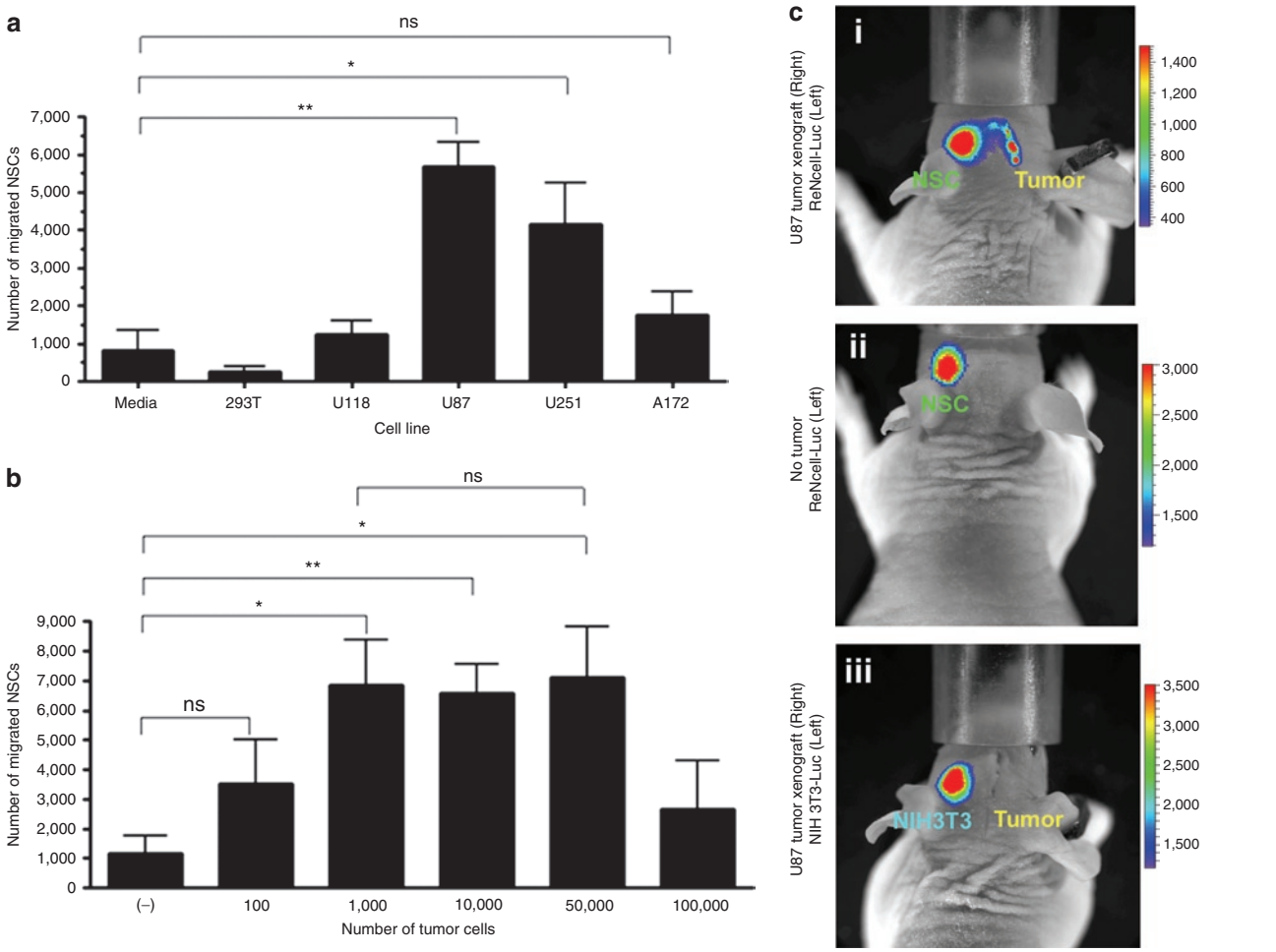

Figure 2 Tropism of neural stem cells (NSCs) for human malignant glioma cells *in vitro and in vivo*. NSC migration in response to different glioma cell lines was evaluated in Transwell migration chamber assay. (**a**) Quantitative measurement of the migrated NSCs in response to a panel of human glioma cell lines. U87 and U251 cells significantly stimulated NSC migration through transwell chambers after a 24-hour incubation ($P < 0.005$ for U87 cell and $P < 0.05$ for U251 cells compared to media alone). (**b**) Number of migrated NSCs in response to different amount of U87 cells. A total of 1,000 U87 cells was the minimum dose able to induce transwell migration of NSC ($P < 0.05$ for 1,000 U87 cells compared to media alone). (**c**) *In vivo* tumor-tropic migration of ReNcell. Bioluminescent imaging of mice after intracranial injection of ReNcell-Fluc into the left hemisphere of the mice implanted with U87 xenograft tumors on the right side 7 days (i) before or (ii) mice with no tumor. Another group of tumor-bearing mice received control fibroblast NIH-3T3-Rluc cell. Each group had five animals; photographs show a representative animal from each group. Imaging was done 24 hours postimplantation of the NSCs.

we observed a decreased intracellular viral titer as the titer of the cell-free viral progeny increased. Taken together, we concluded that one replication cycle for the CRAd-S-pk7 virus in NSCs required about 72 hours and progeny release reached its peak at 96 hours postinfection.

Next, we evaluated whether the therapeutic virus released from the loaded NSCs was able to induce oncolysis as efficiently as when the tumor cells were treated with the virus alone. To test this, we placed a panel of glioma cell lines in the bottom well of a Transwell chamber plate and an equal amount of the CRAd-S-pk7 virus alone or loaded into NSCs (10 I.U. of CRAd-S-pk7 virus per NSC) in the top well. After 6 days of incubation, the viability of the tumor cells was examined by trypan blue exclusion methods. As shown in **Figure 1d**, the oncolytic adenovirus released from the loaded NSCs was able to kill human glioma cells as efficiently as the naked virus treatment.

Tropism of NSCs for different human glioma cell lines *in vitro*

The inherent tumor-tropic property of NSCs is central to their utility as a reliable delivery vehicle for cancer gene therapy. As such, we next evaluated the glioma-specific migratory capacity of our NSCs with an *in vitro* migration assay using transwell plates. Accordingly, red fluorescent–labeled NSCs were placed in the upper wells and glioma cells were cultured in the lower chamber of the transwell migration plate with serum-free media. A semiporous membrane (8-μm pores) separated the chambers. Media supplemented with 10% fetal bovine serum was used as a positive control; serum-free media without any cells and a non-glioma cell line (293T) were used as negative controls. NSCs, when exposed to serum-free media or to 293T cells, displayed very low levels of migration; however, about 30–40% of the total plated NSCs migrated to the bottom chamber within 24 hours of

coculture (**Figure 2a**) when exposed to U87 (**$P < 0.005$ compared with media alone) and U251 (*$P < 0.05$ compared with media alone) cells. The U118 and A172 cells failed to induce significant NSC migration compared to the negative control. These results indicate that NSCs are able to migrate in response to certain human glioma lines *in vitro*. Mechanisms underlying this specificity are currently under investigation.

To examine the minimum number of glioma cells required to initiate tumor cell–specific migration, different numbers of U87 cells were plated in the bottom chamber with a constant number of NSCs in the upper chamber of the transwell plates. We observed that as few as 1,000 U87 glioma cells were able to induce an appreciable level of NSC migration within 24 hours of coculture (*$P < 0.05$; **Figure 2b**) and the number of migrated NSCs remained unchanged with increasing number of U87 cells.

We next evaluated the tumor-specific migratory ability of NSCs *in vivo* by creating a NSC line stably expressing firefly luciferase (ReNcell-Fluc). The ReNcell-Fluc cells were implanted in the left hemisphere of the brains of nude mice bearing a U87 glioma in their right hemisphere (**Figure 2c-i**). The tumor-specific migration of the implanted ReNcell-Fluc was monitored using *in vivo* bioluminescent imaging. As controls, we implanted the fibroblast cell line NIH-3T3 stably expressing Fluc (**Figure 2c-iii**) contralaterally in tumor-bearing animal brains and the ReNcell-Fluc cells were implanted in animals without xenograft tumors. The transplanted ReNcell-Fluc rapidly crossed the midline and migrated to the contralateral hemisphere only in the brain of animals with an established xenograft tumor (**Figure 2c-i**) as early as 16 hours postimplantation (data not shown). We did not observe any migration when ReNcell-Fluc cells were implanted in the animal brain without xenograft tumors (**Figure 2c-ii**). Furthermore, this migration was an NSC-specific phenomena as our control NIH-3T3-Fluc cells did not migrate to the hemisphere with established tumors (**Figure 2c-iii**). These observations indicate that NSCs migrate selectively toward glioma in an *in vivo* xenograft tumor model.

Effect of oncolytic virus loading on tumor-tropic migration of NSCs *in vitro*

We next determined the maximum loading dose of CRAd-S-pk7 virus possible for NSCs without negatively affecting their tumor-tropic migration. The NSCs were loaded with increasing doses of CRAd-S-pk7 (1.0–100.0 I.U./NSC) virus and evaluated for their migration toward U87 glioma cells. Surprisingly, we observed a significant improvement in tumor-tropic migration of the NSCs after loading with the oncolytic virus regardless of the loading doses at 24 hours postincubation (**Figure 3a-i**). The number of migrated cells almost doubled after loading with 10 I.U. of CRAd-S-pk7 viruses per NSC (*$P < 0.05$ compared to uninfected control). However, the magnitude of difference in number of migrated cells decreased over time (**Supplementary Figure S3**). This is possibly due to the cytopathic effects of CRAd-S-pk7 on the carrier cells treated with the higher loading/infection doses as reported in our previous experiments. We next examined our observations in the orthotopic glioma model *in vivo* by implanting ReNcell-Fluc with or without CRAd-S-pk7 virus loaded into the cerebral hemispheres of mice contralateral to established U87 xenograft tumors. As shown in **Figure 3a-ii**, ReNcell-Fluc loaded with the oncolytic virus were able to cross the midline and migrate to the tumor-bearing contralateral hemisphere with much faster kinetics as compared to NSCs alone.

Next, we investigated the possible molecular mechanisms behind CRAd-S-pk7-mediated enhancement of NSC's tumor-tropic migration by monitoring relative transcription levels of chemokine receptors using quantitative RT-PCR (qRT-PCR). We observed about a tenfold upregulation of *CXCR4*, a 15-fold increase in *c-MET* and a twofold increase in the *VEGFR2* expression at 32 hours postloading (**Figure 3b**). Next, we evaluated the upregulation of the chemoattractant receptors at the protein level following oncolytic adenovirus loading by fluorescence-activated cell sorting. As a control, we infected NSCs with a replication-incompetent adenovirus (Ad-pk7-Luc), which contains identical surface modifications as our oncolytic CRAd-S-pk7 virus, but lacks the E1A gene that is essential for replication. Both viruses were able to increase CXCR4 expression as compared to their uninfected counterpart at 24 hours postinfection (**Figure 3c-i**). This increase in CXCR4 expression at the protein level was observed and presented as percent of positive cells in the total infected NSC population (**Figure 3c-i**) and the CXCR4 expression per cell base (mean fluorescence intensity; **Figure 3c-i,ii**) and remained elevated 48 hours postinfection (**Figure 3c-ii**). However, only the oncolytic adenovirus was able to enhance the VEGFR2 expression following infection (**Figure 3c-i, bottom row & ii**). We did not observe any correlation between the transcript and protein level for the c-Met receptor.

To determine whether CXCR4 and VEGFR2 signaling molecules were necessary for the enhancement in the NSC's migratory ability after oncolytic adenovirus loading, we performed functional blocking of CXCR4 and VEGFR2 receptors in cell migration assays. The neutralizing antibodies to these receptors inhibited the glioma-specific migratory capacity of NSCs about 60% after adenovirus loading as compared to their corresponding IgG control group (**Figure 3d**). This inhibition was further enhanced when neutralizing antibodies were combined. Taken together, these data suggest that oncolytic virus loading/infection significantly improves migratory capacity of NSCs toward brain tumor cells and also increases the expression of chemoattractant receptors such as CXCR4 and VEGFR2, which have been reported to be involved in the migration process of NSCs.[11]

Oncolytic virus–loaded NSCs produce more therapeutic virus both *in vitro* and *in vivo*

We then determined the optimal loading/infecting dose that would result in maximal production of therapeutic virus by NSCs. The total amount of CRAd-S-pk7 virus released from the NSCs at 72 hours after loading was obtained by measuring the viral progeny and *E1A* copy number in the U87 cells plated at the bottom of the migration chamber. As shown in **Figure 4a,b**, the maximum amount of viral progeny released from the carrier cells was attained after loading with the dose of 50 I.U. per NSC ($P < 0.0005$ compared to 1.0 I.U.). Both 10 and 50 I.U. loading doses were able to produce about 1×10^9 I.U (**Figure 4a**) total viral progeny, but the viral DNA replication measured by E1A copies was about 2 log

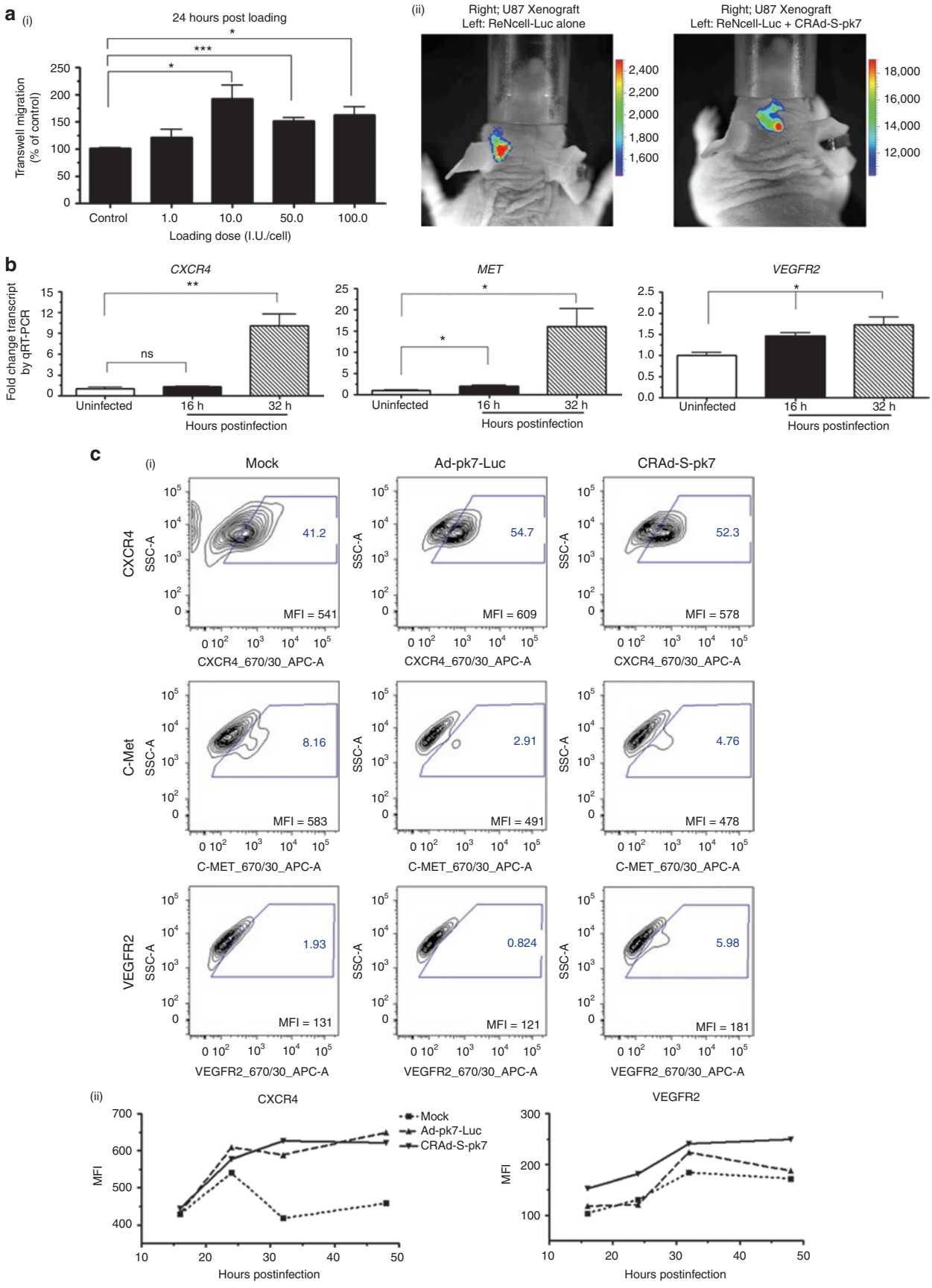

Figure 3 Continued on next page

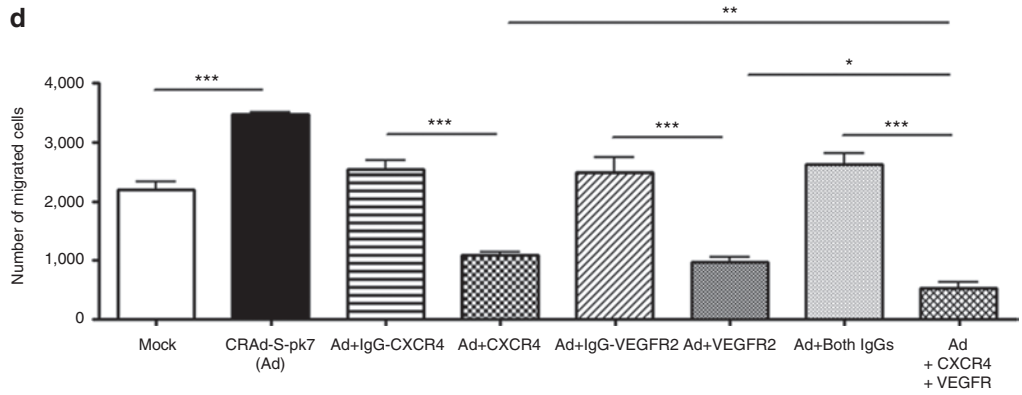

Figure 3 Oncolytic virus loading into neural stem cells (NSCs) augments their tumor-tropic migration *in vitro*. (**a**-i) Tumor-tropic migration of CRAd-S-pk7 loaded NSCs in response to U87 cells 24 hours after coculture in the transwell plate. All conditions were conducted in quadruplicate and repeated in two separate experiments. CRAd-S-pk7 significantly enhanced the *in vitro* tumor-tropic migration of NSCs. (**a**-ii) *In vivo* tumor-tropic migration of ReNcell after loading with CRAd-S-pk7 [50 infectious unit (I.U.)/cell]. Bioluminescent imaging of mice after intracranial injection of ReNcell-Fluc with (right) or without (left) CRAd-S-pk7 into the left hemisphere of the mice previously implanted with U87 xenograft tumors. Each group had five animals and a representative photograph is shown from each group. Imaging was done 8 hours postimplantation of the NSCs. (**b**) Analysis of expression of chemoattractant receptors c-MET, CXCR4, and VEGFR2 expression postloading with 50 I.U. of CRAd-S-pk7 virus per NSCs by quantitative RT-PCR (qRT-PCR); $^{*}P < 0.05$, $^{**}P < 0.005$ versus uninfected control. (**c**) Fluorescence-activated cell-sorting (FACS) analysis indicating that loading oncolytic adenovirus into ReNcell upregulates CXCR4 and VEGFR2 expression. ReNcell were infected with 50 I.U./cell of oncolytic adenovirus CRAd-S-pk7 (right column) or replication-incompetent Ad-pk7-Luc (middle column) and FACS analysis was performed at 16, 24, 32, and 48 hours postinfection. Cells were gated on isotype control and analyzed for CXCR4, c-Met, and VEGFR2 expression. (i) Representative contour plot profiles of chemoattractant receptor expression after 24-hour infection with the different viruses. The mean fluorescence intensity (MFI) of the total population is indicated in the contour plots (a representative experiments is shown; $n = 4$). (ii) CXCR4 and VEGFR2 receptor expression kinetics in the ReNcells after infection with different adenovirus expressed as MFI at 16, 24, 32, and 48 hours postinfection. A representative experiment of the four is shown. (**d**) Adenovirus infection/loading-induced enhancement of migratory capacity of ReNcell is blocked by function-inhibiting antibodies. ReNcells were incubated with CRAd-S-pk7 (50 I.U./cell) for 1 hour and preincubated with CXCR4 and VEGFR2 receptor function-inhibiting antibodies or isotype-matched control (IgG-CXCR4 and IgG-VEGFR2) antibodies for 1 hour, and then the cells were allowed to migrate to U87 cells in the transwell plate assay as described in the method section; experiment was done in triplicate, bars, SD. $^{***}P < 0.0001$. Similar data were obtained in three independent experiments.

higher when NSCs were loaded with 50 I.U. of CRAd-S-pk7 virus per NSCs (**Figure 4b**). At the loading dose of 100 I.U. per NSC, the production of viral progeny decreased significantly, likely due to oncolytic virus–induced toxicity on producer cells. Based on these data, we decided to evaluate the loading doses of 10 and 50 I.U per NSC for all future *in vivo* experiments.

To evaluate whether CRAd-S-pk7-loaded NSCs can act as *in situ* virus factories and sustain a high dose of therapeutic virus at the tumor site as compared to treatment with naked virus, we first plated U87 glioma cells at the bottom chamber of the transwell plate. Equal amounts of the CRAd-S-pk7 virus (1×10^6 I.U.) alone or loaded into NSCs (2×10^4 NSCs loaded with 50 I.U./cell of CRAd-S-pk7 virus) were placed in the upper chamber. The tumor cells from the bottom chamber were harvested every day for 6 days and assayed for viral titer. As shown in **Figure 4c**, NSCs loaded with the CRAd-S-pk7 virus maintained three- to fourfold more viral progeny as compared to the group treated with virus alone at day 4 and 5 after coculture ($^{***}P < 0.0005$).

Next, we examined this phenomenon *in vivo* by implanting U87 cells into the right hemisphere of athymic nude mice. Seven days after tumor implantation, a single intratumoral injection of the CRAd-S-pk7 virus (2.5×10^7 I.U.) alone or loaded into NSCs (5×10^6 NSCs loaded with 50 I.U./cell of CRAd-S-pk7 virus) was administered. Animals were killed at 3, 7, and 14 days after virus injection, and the tumor-containing right hemisphere of each animal was harvested and assayed for viral titer. We observed that the group of animals ($n = 3$) that received virus loaded into NSCs contained about fivefold more virus as compared to the virus alone per mg of tissue ($^{**}P < 0.005$ with virus-alone injected group; **Figure 4d**) at 3 days after virus injection. At day 7, we were able to recover a detectable amount of virus from two out of three animals in the same group, whereas viral progeny was recovered from only one animal in the group that received CRAd-S-pk7 virus alone (**Figure 4d**). These data indicate that the NSCs loaded with oncolytic virus can function as virus factories and are able to facilitate the maintenance of a higher viral titer over time both *in vitro* and *in vivo*.

NSCs decrease CRAd-S-pk7-induced astroglial and microglial activation

The host immune response against therapeutic oncolytic viruses is considered one of the major obstacles to the successful application of this approach in the clinic.[12,13] The immunosuppressive properties of NSCs are well documented both *in vitro* and in *in vivo* animal models.[12–14] Taken together, we hypothesized that loading oncolytic adenovirus into NSCs may reduce the host immune activation in response to the therapeutic virus. To test this hypothesis, we injected naked CRAd-S-pk7 virus or virus loaded into human NSCs in the brains of nude mice and killed animals at 7 and 14 days following treatment to evaluate immune activation. Assessment of neuronal damage was first undertaken in sections stained with hematoxylin–eosin at 14 days after various treatments (**Figure 5a-i–iii**). The group of animals that received oncolytic virus alone showed extensive neuronal loss and necrosis at the injection site (**Figure 5a-ii**) as compared to phosphate-buffered saline (PBS)–treated animals (**Figure 5a-i**). We did observe some

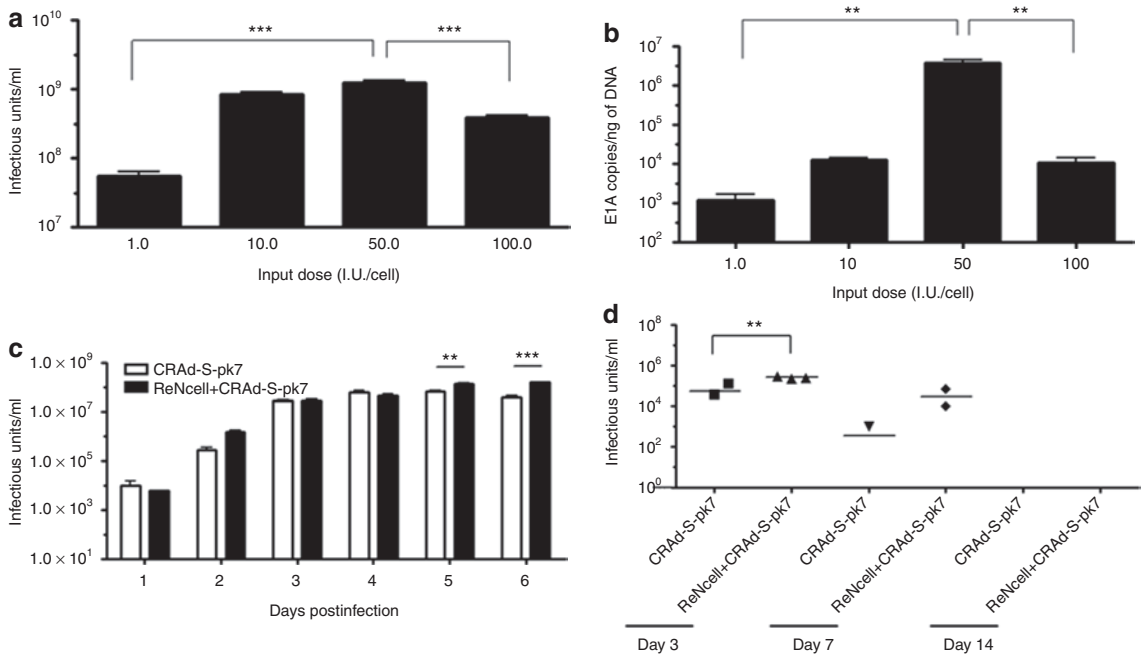

Figure 4 Neural stem cells (NSCs) can act as *in situ* virus factories and maintain high doses of therapeutic virus *in vivo*. (**a**) U87 cells at the bottom wells from the Transwell migration experiments were collected at 72 hours along with the media and the CRAd-S-pk7 virus titer was measured. NSCs loaded with 50 infectious units (I.U.) of CRAd-S-pk7 per NSC were able to hand off maximum amount of therapeutic virus to the target tumor cells (error bars are SD; $P < 0.0005$ at loading dose of 50 I.U.), but the virus titer decreased when NSCs were loaded with 100 I.U. of CRAd-S-pk7 virus per cell ($P < 0.0005$ compared to loading dose of 50 I.U.). (**b**) The replicative capacity of CRAd-S-pk7 virus measured by quantitative RT-PCR in the targeted U87 cells. The extent of viral replication was determined by measuring the number of viral E1A copies per ng of DNA (error bars are SD). At the loading dose of 50 I.U. per NSC, the carrier cells were able to deliver the maximum amount of oncolytic virus to the target tumor cells as shown by the E1A copy number/ ng of DNA ($P < 0.005$ compared to loading dose 1.0 I.U./NSC). (**c**) This experiment was performed as described in the previous experiments (**Figure 1b**) but only using the U87 cells line. U87 cells at the bottom wells were collected every day along with the media for 6 days and the titer of CRAd-S-pk7 was measured. At day 5 and 6, the NSCs loaded with CRAd-S-pk7 virus were able to sustain a high titer of therapeutic virus in the target U87 cells (error bars are SD; $P < 0.005$ at day 5 and $P < 0.0005$ at day 6 compared to virus alone). (**d**) *In vivo* evidence that NSCs loaded with CRAd-S-pk7 virus can sustain high level of therapeutic virus titer. Mice were implanted with 2.5×10^5 U87 cells in the right frontal lobe and the tumors were allowed to grow for 7 days. CRAd-S-pk7-loaded NSCs (5×10^5 cells loaded with 50 I.U. of CRAd-S-pk7/NSC or equal amount of naked virus) were then injected intratumorally. Mice were killed at indicated time points, tumor from each animal was harvested and measured for virus titer ($n = 3$; student *t*-test, $P < 0.005$ at day 3).

degree of neuronal loss at the injection site when the oncolytic adenovirus was delivered *via* NSCs (**Figure 5a-iii**); however, the extent of tissue loss in this group of animals was much less pronounced than the oncolytic virus–alone group. We also stained sections of the same animal brains from the various treatment groups with glial fibrillary acidic protein (GFAP), a well-known marker of glial cell activation in response to neuroinflammation[15] (**Figure 5a-iv–vi**) and major histocompatibility complex (MHC) class II (**Figure 5a-vii–ix**) and observed that the animals which received oncolytic adenovirus alone had higher numbers of GFAP and MHC class II immunoreactive cells at the injection sites versus animals that received oncolytic virus loaded into NSCs.

Response to these treatments was also evaluated by fluorescence-activated cell sorting analysis of GFAP-positive cells following homogenization of injected brains. We observed no difference between the groups of animals that were injected with the virus alone or the virus loaded into NSCs with regard to the percent of GFAP-positive cells at 7 days postinjection (**Figure 5b,c**). However, at 14 days after injection, we observed 3 times more GFAP-positive cells in the group that received virus alone as compared to the group that received virus loaded into NSCs (**Figure 5b**,$^{**}P < 0.005$ compared to virus-alone group). We did not observe any statistically significant difference in the average percent of infiltrating $CD11b^{+}/CD45^{high}$ bone marrow–derived macrophages between the two groups (**Supplementary Figure S2**). Therefore, delivery of oncolytic virus in the brain loaded into NSCs reduced the activation of the resident microglia and astrocytes in response to adenoviral vector, but did not appear to affect the recruitment of bone marrow–derived macrophages.

To elucidate the mechanisms behind the NSC-mediated inhibition of astroglial activation, we examined innate immune modulators involved in response to adenovirus infection by qRT-PCR in NSCs. Adenovirus infection induces the expression of numerous genes associated with the innate immune responses in the target cells including interleukin-6 (IL-6), tumor necrosis factor α (TNF-α), interferon-γ, monocyte chemoattractant protein-1, and RANTES within a few hours of infection.[16] As shown in **Figure 5d**, proinflammatory cytokines such as IL-6 and TNF-α were significantly upregulated at 16 and 32 hours, respectively, in response to CRAd-S-pk7 loading/infection into NSCs. We also observed, very surprisingly, that the adenovirus increased expression of the anti-inflammatory cytokine IL-10 about tenfold at 16 hours after loading. We further evaluated IL-10 expression at the protein level by enzyme-linked immunosorbent assay and observed that IL-10

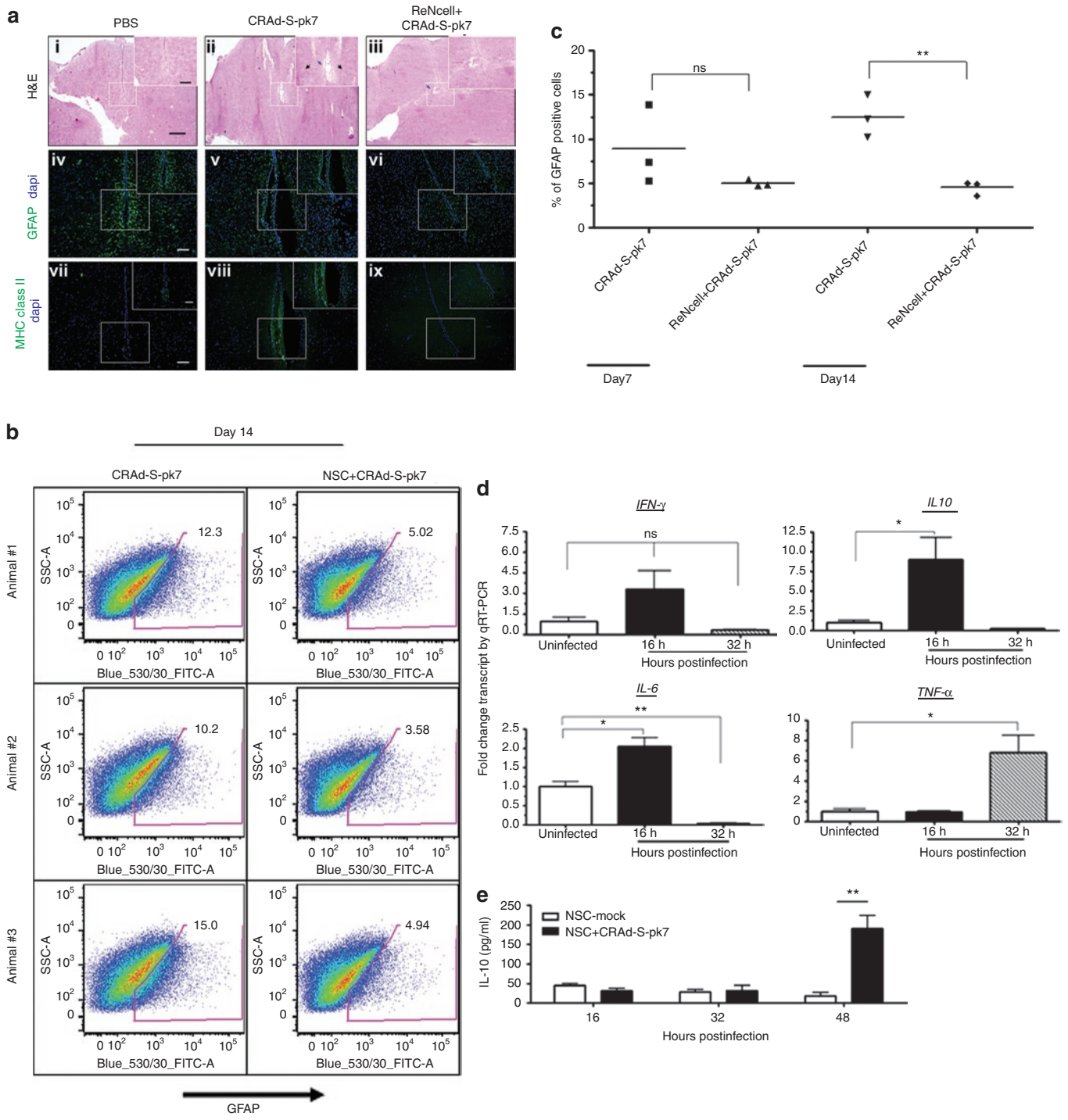

Figure 5 Inhibitory effects of neural stem cells (NSCs) on adenovirus-induced neuroinflammation. (**a**) Evidence of brain damage in the injection sites. Histological features of brains from mice injected with CRAd-S-pk7 virus alone (2.5×10^7 I.U./ injection) or virus loaded into NSCs (5×10^5 cells loaded with 50 I.U. of CRAd-S-pk7 per NSCs) harvested at day 7 and 14 postinjection. (i–iii) Low-magnification image of hematoxylin–eosin (H&E) staining assessing neuronal toxicity postinjection. Bars = 80 µm. In box, high-magnification microphotograph show neuronal loss (blue arrow) and immune infiltrates (black arrow) at the site of injection. Bars = 40 µm. Representative image of sections of the same animal brain as H&E sections stained with anti-glial fibrillary acidic protein (GFAP) (iv–vi) and anti-mouse MHC class II antibody (vi–ix). Bars = 100 µm. (**b**) Brains from mice injected with CRAd-S-pk7 virus alone (2.5×10^7 I.U./injection) or virus loaded into NSCs (5×10^5 cells loaded with 50 I.U. of CRAd-S-pk7 per NSCs) harvested at day 7 and 14 postinjection. Percent of GFAP-positive cells was measured by fluorescence-activated cell sorting from the injected brains. Animals receiving virus loaded into NSCs showed significant decrease in % GFAP-positive cells in the brains compared to the group that received virus alone. (**c**) Percent of GFAP-positive cells was significantly decreased in the mouse brains injected with CRAd-S-pk7 loaded NSCs; $^{**}P < 0.005$ versus CRAd-S-pk7 alone group at day 14 postinjection. (**d**) Analysis of expression of innate immune response genes expression post loading with 50 I.U. of CRAd-S-pk7 virus per NSCs by quantitative RT-PCR (qRT-PCR); (**e**) IL-10 production by NSC infected with CRAd-S-pk7 virus (50 I.U./cell). ELISA was performed for the quantification of the cytokines on the cell culture supernatant; $^{**}P < 0.005$ in comparison with the uninfected NSCs.$^{*}P < 0.05$, $^{**}P < 0.005$ versus uninfected control. GFAP, glial fibrillary acidic protein; PBS, phosphate-buffered saline.

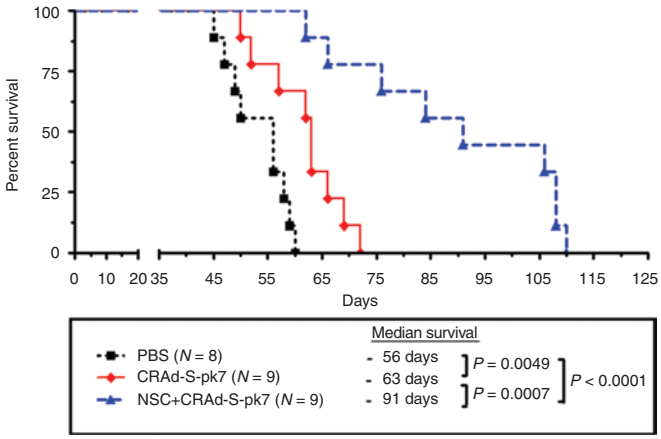

Figure 6 Oncolytic virus–loaded neural stem cells (NSCs) inhibit xenograft growth and prolong survival of mice with orthotopic glioblastoma. 2.5×10^5 U87 cells were injected stereotactically into the right hemisphere of the brains of 9- to 12-week-old *nu/nu* mice followed by intratumoral (IT) injection of CRAd-S-pk7 alone (2.5×10^7 I.U./animal) or loaded into NSCs (5×10^5 NSC/animal loaded with 50 I.U./NSC, total 2.5×10^7 I.U. viral dose) at 5 days after tumor implantation. The median survival was 56 days in group receiving phosphate-buffered saline (PBS) injection compared with 63 days in the group treated with virus alone and 93 days in the group treated with NSCs loaded with oncolytic virus, $n = 9$, [log-rank, PBS versus CRAd-S-pk7 (2.5×10^7 I.U.), $P = 0.0049$; PBS versus ReNcell + CRAd-S-pk7 (5×10^6 I.U.), $P < 0.0001$; CRAd-S-pk7 versus ReNcell + CRAd-S-pk7 (2.5×10^7 I.U.), $P = 0.0007$].

expression was significantly upregulated in the NSCs infected with CRAd-S-pk7 at 48 hours postinfection (**Figure 5e**). Taken together, these results indicate that loading of CRAd-S-pk7 into NSCs leads to the expression of both pro- and anti-inflammatory genes and decreases adenovirus-mediated neuroinflammation.

Oncolytic virus–loaded NSCs inhibit xenograft growth and prolong survival of mice with orthotopic glioblastoma

Finally, we evaluated the therapeutic potential of oncolytic virus–loaded NSCs in an orthotopic glioma model (**Figure 6**). Five days following tumor implantation, animals were randomly divided into separate groups and treated with CRAd-loaded NSCs (2.5×10^7 I.U. total/mouse = loading dose 50 I.U./cell of oncolytic virus loaded into 5×10^5 of carrier cells), an equal dose of CRAd-S-pk7 alone (2.5×10^7 I.U. total/mice), or control. As a control, we injected equal volumes of PBS and the same number of NSCs without the therapeutic virus intratumorally. Mice treated with NSCs alone displayed similar survival to the PBS-treated control group (data not shown). About 50% of the animals from the group treated with NSCs loaded with CRAd-S-pk7 virus (50 I.U./cell loading dose) survived beyond 100 days, whereas none of the animals in the group treated with CRAd-S-pk7 virus alone survived beyond 75 days. We also observed a significant improvement in median survival from 63 to 93 days (~50%) between these two groups ($P = 0.0007$). These results indicate that CRAd-S-pk7-loaded NSCs effectively deliver oncolytic adenovirus to malignant glioma *in vivo* resulting in a significant inhibition of tumor growth with a simultaneous increase in the median survival of treated animals as compared to CRAd-S-pk7 treatment alone.

DISCUSSION

The concept of our study is based on the fact that NSCs possess inherent tumor-tropic properties, which provides a novel platform for anticancer therapy that may be harnessed to selectively target and deliver therapeutic payloads such as oncolytic adenovirus to invasive tumor burdens. It has been shown that oncolytic viruses can selectively infect and kill glioblastoma both in the preclinical setting as well as recent clinical trials.[17,18] Despite successes, the therapeutic efficacy of this approach in the clinic has been hampered by the inability of currently available therapeutic vectors to target the diffuse topography characteristic of brain tumors effectively due to the rapid host immune response mounted against the viral vector.[19] Previously, we have reported the use of NSCs as a cell carrier to enhance intratumoral distribution of an oncolytic adenovirus in an orthotopic model of malignant glioma.[9] In this study, we have shown for the first time that an immortalized NSC line loaded with an oncolytic adenovirus CRAd-S-pk7 can effectively suppress tumor growth in an orthotopic intracranial xenograft model of human malignant glioma and prolong animal survival.

One of the important requirements for an ideal cell carrier system for oncolytic virus delivery is that the carrier cell must be permissive to the virus while supporting viral replication effectively.[10] We found that the oncolytic adenovirus CRAd-S-pk7 was able to infect the carrier NSCs efficiently; additionally NSCs can support viral replication over time. One of the challenges of such a delivery system is that loading NSCs with a replication-competent viral vector eventually lyses the carrier cells. This is an essential step for the site-specific amplification of the therapeutic vector, but counterproductive for the long-term survival and tumor-specific homing of the carrier cells, partly because premature lysis of NSCs will reduce the dose of the therapeutic payload that ultimately reaches target sites. With this in mind, our *in vitro* loading optimization experiments identified the loading dose of 10 and 50 I.U. of CRAd-S-pk7 virus per carrier cell that resulted in moderate cytolysis of the carrier cells, yet effectively lysed glioma cells (**Figure 1a,d**). Moreover, NSCs loaded with the CRAd-S-pk7 virus were able to sustain elevated levels of therapeutic viral titer over time compared to when the virus was delivered alone (**Figure 4c,d**). These data support the notion that NSCs can be harnessed as virus-producing factories to maintain high doses of oncolytic virus at target sites. The successful clinical translation of such delivery system will require additional modifications that will reduce the lytic activity of the conditionally replicating vector specifically in carrier cells in order to prolong their survival and allow them to home to satellite tumor masses more efficiently.

The ability of NSCs to travel great distances throughout the brain and migrate to the disseminated tumor burden is central to their utility as cellular vehicles for targeted antiglioma therapy.[11,20] We observed that NSCs preferentially migrate in response to certain human glioma cell lines such as U87 and U251, but are much less responsive to other lines (U118 and A172; **Figure 2a**). The different tumor-tropic migratory cue(s) provided by different glioma cell lines are probably responsible for such specificity and require further investigation. The minimum number of tumor cells required to induce tumor-tropic migration *in vitro* was 1,000 and total migration plateaued at this dose, potentially indicating

saturating concentrations of promigratory cues. The tumor-specific migratory properties of ReNcells were also evaluated in an orthotopic xenograft model (**Figure 2c**). We estimated that about 20–30% of NSCs migrated in response to glioma cells within the first 24 hours and that number remained unchanged over time (**Figure 2b,c**). It is conceivable that only certain subpopulation(s) of NSCs are capable of tumor-tropic migration. Further characterization of such populations will allow us to maximize the number of cell carriers able to home to metastatic tumor burdens.

One of our major concerns in loading oncolytic adenovirus into NSCs was how infection would affect the tumor-tropic migratory ability of the carrier cells. Surprisingly, we observed that at 24 hours postloading with the CRAd-S-pk7 virus, NSCs migrated more efficiently than the uninfected control *in vitro*. Next, we examined this observation in an orthotopic xenograft model by implanting NSCs loaded with or without CRAd-S-pk7 in the hemisphere contralateral to tumors. The NSCs loaded with oncolytic virus were able cross the midline and migrate towards the tumor implanted hemisphere whereas their noninfected counterpart remained fixed at its inoculation site (**Figure 3a-ii**). At the loading dose of 10 I.U. per NSC, the migration of NSCs in response to human glioma was almost doubled *in vitro* (**Figure 3a**). However, the number of migrated cells decreased at higher loading doses (50 and 100 I.U./NSC; **Figure 3a**), probably due to the lytic activity of the loaded therapeutic virus. The *in vivo* consequences of the oncolytic adenovirus loading on the tumor-tropic migration of NSCs are currently under investigation.

Numerous cytokines, growth factors, and their receptors have been implicated in the tumor-homing properties of NSCs, including SCF/c-Kit,[21] SDF1/CXCR4,[22] HGF/c-Met,[23] VEGF/VEGFR,[24] and monocyte chemoattractant protein-1/CCR2.[25] Based on the concept that the cytokine–chemokine interaction regulates the tumor-tropic migration of NSCs, we next investigated the possible mechanisms underlying adenovirus-mediated enhancement of NSC migration by monitoring the expression of different chemoattractant receptors using qRT-PCR. We found that the expression of chemokine receptors CXCR4, c-Met, and VEGFR2 significantly increased at the mRNA level in NSCs (**Figure 3b**). However, only CXCR4 and VEGFR2 receptor expression was elevated at the protein level within 16 hours of loading with the CRAd-S-pk7 virus (**Figure 3c**). This tumor-specific enhancement of migratory capacity can be partially inhibited by the blocking antibody against each of these receptors independently with synergy between the two when applied together (**Figure 3d**). This is an unexpected finding because it has been previously reported that adenovirus E4 protein is a potent inhibitor of CXCR4 expression[26] and the CRAd-S-pk7 virus used in this study contained an intact E4 region of the viral genome. Moreover, the induction of this receptor was very rapid after adenovirus exposure and both the replication-incompetent and the replication-competent adenovirus were able to induce receptor expression to the same extent, which led us to speculate that this may be part of NSC's innate antiviral immune response. On the other hand, only replication-competent oncolytic virus loading onto NSCs upregulated VEGFR2 expression.

The *ex vivo* loading of therapeutic virus into carrier cells must be synchronized with the timing of *in vivo* delivery to achieve an optimal dose of the oncolytic virus at tumor sites.[10] Thus, the kinetics of the replication of therapeutic virus within carrier cells will play a critical role in achieving optimal *in vivo* delivery. With this in mind, our virus-titering experiments indicated that each NSC produced about 2,000 virions in 72 hours after infection with 50 I.U. of oncolytic virus. The CRAd-S-pk7 virus required ~72–96 hours to complete one cycle of replication in the NSCs. Maximum release of the progeny from the carrier cells was obtained at 4 days postloading. We previously showed that a single intratumoral injection of 1×10^9 viral particles of CRAd-S-pk7 delayed the growth of glioma in our orthotopic animal model.[27] Our data indicated that about 5×10^5 carrier cells loaded with 50 I.U./cell of the oncolytic virus should be able to obtain such level of therapeutic viral dose at the target sites.

A wealth of preclinical data suggests that *in vivo* transplanted NSCs can act as immunosuppressants.[12,13] This immunosuppressive quality of NSCs is a very attractive attribute for a cell carrier given that NSCs can suppress the immune system locally at delivery sites, thus allowing the therapeutic oncolytic virus to replicate longer and kill tumor cells without much immune interference. To investigate how the immunosuppressive properties of NSCs can alter the adenovirus-mediated neuroinflammation, alternative immune indicators needed to be employed as nude mice do not have all the components of the normal immune system (lacking T and B cells). Our initial immunohistochemical analysis of the injection sites indicated that oncolytic adenovirus alone induced more pronounced neuronal loss and tissue damage (**Figure 5a-i,ii**), which was also accompanied by higher immunoreactivity based on the expression of GFAP (**Figure 5a-iii–vi**) and MHC class II (**Figure 5a-vii–ix**) molecules as compared to animals that received CRAd-S-pk7 virus loaded into NSCs. This pattern of immune activation is also observed in pathological instances such as AIDS dementia,[28] central nervous system–related inflammation and other viral infections.[29] The increase in the expression of GFAP and MHC class II is one of the earliest responses to central nervous system injury and is associated with reactive astrogliosis.[30] It has been previously reported that adenoviral vectors injected into the central nervous system induce a strong inflammatory response, which is associated with astroglial activation and associated GFAP upregulation.[15] Based on this, we examined CRAd-S-pk7-mediated neuroinflammation and astrogliosis with or without loading into NSCs by monitoring the percent of GFAP-positive cells in the brain of the injected animals over time. Our preliminary data showed that adenovirus alone can increase GFAP immunoreactivity in animal's brains at 14 days postinoculation and that GFAP expression was significantly decreased when the virus was delivered loaded into NSCs. It has been demonstrated that the virus induced proinflammatory cytokine IL-6 is a key mediator for astrogliosis in the *in vivo* rat model.[31] Adenoviral vectors can induce potent innate immune responses and increase serum IL-6, TNF-α, and IL-12 within hours of infections in a dose-dependent manner.[16] It is, therefore, conceivable that the increased GFAP and MHC class II expression we observed in the group of animals that received naked CRAd-S-pk7 virus was possibly due to the innate immune induction and production of proinflammatory cytokines such as IL-6 by the vector in the brain. At the same time, anti-inflammatory cytokines such as IL-10 decrease GFAP expression and suppress IL-6 triggered gliosis.[31]

To understand the mechanisms of NSC-mediated suppression of GFAP expression, we monitored the innate immune response following adenovirus infection/loading in the NSCs by qRT-PCR. As expected, the mRNA levels of the proinflammatory cytokines such as IL-6 and TNF-α were elevated by CRAd-S-pk7 infection (**Figure 5c**). However, we also observed induction of immunosuppressive cytokines such as IL-10, which was upregulated about five-fold as compared to uninfected NSCs. Recently, Woiciechowsky et al. reported that IL-10 could suppress IL-6-induced GFAP expression and gliosis in a dose-dependent manner.[31] Therefore, IL-10 induced by the infected NSCs may act as neuroprotectant and suppress adenovirus-induced GFAP expression and neuroinflammation. We would attribute the production of these cytokines to resident cells in the brain or the implanted NSCs as we did not observe any difference in the percent of peripherally derived immune cells in the brains of animals in different groups (**Supplementary Figure S2**). For the future, the immunosuppressive properties of NSCs with respect to their utility as a cell carrier for oncolytic virus must be carried out in immunocompetent and permissive animal models such as the cotton rat.

An important safety issue for the clinical use of NSC as a cell carrier is the question of their contribution to oncogenesis. We found that the animals from the group treated with NSCs alone expire at the same time as the PBS-treated control group. Our data corroborate with previous reports showing that intratumoral injection of immortalized human NSC lines did not accelerate tumor growth *in vivo*.[11] Even though our *in vitro* optimization experiments identified the optimal loading dose of 10 I.U. per NSCs with respect to both the viability of the carrier cells and the production of the therapeutic viral progeny, only when NSCs were loaded with 50 I.U./NSC was a significant improvement in median survival observed. Median survival of the animals treated with NSC-loaded CRAd-S-pk7 was improved by about 30 days as compared to virus-alone group (**Figure 6**). Some potential limitations of the survival experiments presented in this study include the intratumoral administration of the oncolytic therapy and the use of a single tumor cell line to evaluate the therapeutic efficacy. Before NSCs can be considered for use as a cellular vehicle for the delivery of oncolytic virus, this approach must be vigorously evaluated to target and deliver oncolytic virus to disseminated tumor burdens after systemic, nonintratumoral administration.

In conclusion, we show that an immortalized NSC line can be used as a cell carrier to deliver oncolytic adenovirus in an orthotopic glioma model and is able to significantly improve median survival compared to treatment with virus alone. Our findings suggest, for the first time, that the tumor-tropic migratory properties of NSCs are not only sustained after loading with an oncolytic adenovirus, but are also considerably enhanced. This is an important observation for translational purposes due to the extensively invasive nature of human gliomas. However, it remains to be seen whether NSCs loaded with oncolytic virus can effectively target invasive tumor *in vivo* when administered at a distance from the tumor site(s). Also, further characterization of the molecular nature of NSC-mediated immunosupression and how it may help to enhance the therapeutic efficacy of oncolytic adenovirus will reinforce the case for the use of NSCs as a bona fide cell carrier system for antiglioma gene therapy.

MATERIALS AND METHODS

Cell culture and establishment of fluorescent-labeled cell lines. The U87MG, U251MG, U118MG, and A172 human glioma cell lines, A549 and 293T cell line were purchased from the American Tissue Culture Collection (Manassas, VA) and maintained according to vendor recommendations. U87MG cells, U118MG cells were cultured in minimum essential medium (HyClone; Thermo Fisher Scientific, Waltham, MA) and U251MG and A172 cells were cultured in Dulbecco's modified Eagle's medium containing 2% penicillin–streptomycin antibiotic (Cellgro; Mediatech, Manassas, VA) and 10% fetal bovine serum (Atlanta Biologicals, Lawrenceville, GA). All cells (including NSCs) were grown in a humidified atmosphere, with 5% CO_2 and 37 °C conditions. All the lines were subcultured for experimentation using 1 ml/10^6 cells 0.25% trypsin/2.21 mmol/l EDTA solution (cat. no. 25-053-CI; Mediatech). Trypsin activity was quenched using the appropriate media for each cell type. Cells were then washed at 300 relative centrifugal forces and plated at the indicated densities.

Human NSCs (ReNcell) were obtained from Millipore (Temecula, CA) and maintained according the manufacturer's protocol. Briefly, these NSCs were isolated from the cortical region of 14-week-old fetal tissue and immortalized by retroviral transduction and insertion of the *c-myc* gene. Cells were characterized according to their expression of nestin, SOX-2, CD133, and CD44 (data not shown) stem cell markers. Subcultures of human NSCs for experimentation were conducted as follows: tissue culture plastic dishes were coated with laminin (Sigma-Aldrich, St Louis, MO) at a concentration of 20 µg/ml in serum-free Dulbecco's modified Eagle's medium in 37 °C and 5% CO_2 atmospheric conditions 4 hours before NSC plating. NSCs were detached from plastic dishes using 1 ml/10^6 cells of Accutase (Millipore), centrifuged at 300 relative centrifugal forces for 5 min, resuspended in ReNcell NSC Maintenance Medium (Millipore), supplemented with 20 ng/ml basic fibroblast growth factor (Millipore) and 20 ng/ml epidermal growth factor (Millipore), and seeded at the indicated cell densities.

The stable, fluorescently labeled cell lines, ReNcell-mCherry and ReNcell-Fluc were established as follows. Briefly, cells were seeded at a density of 5×10^4 cells/well (or 50–60% confluency) in six-well plastic culture dishes (Becton Dickinson, Franklin Lakes, NJ). One day after plating, cells were incubated for 24 hours with replication-deficient lentiviral vectors containing mCherry or F-luciferase expression cassettes. After 48 hours, media was replaced with fresh culture media appropriate for each cell type containing 1 µg/ml puromycin (Sigma-Aldrich) for the establishment of stable clonal populations.

Viral vector. The replication-competent adenoviral vector CRAd-S-pk7 contains the wild-type adenovirus replication protein, *E1A*, under the control of human *survivin* promoters. These vectors have been created by homologous recombination using a shuttle plasmid containing the human *survivin* promoter upstream of the viral *E1A* gene. Shuttle plasmids containing these regions were further homologously recombined into adenoviral plasmids modified to contain a polylysine (pk7) incorporation into the C-terminus of the wild-type fiber protein.[17,32]

Analysis of viral replication. To detect the level of viral replication by quantitative PCR, NSCs were plated at a density of 2.5×10^4 cells/well in 24-well plastic tissue culture dishes. The next day, cells were infected with indicated I.U./cell of CRAd-S-pk7. After a 1-hour incubation period, virus-containing media were removed, cells were washed with PBS, and a fresh portion of complete growth media was added. Infected cells were harvested at indicated time points. Total DNA was extracted from infected cells using a DNeasy Tissue Kit (Qiagen, Hilden, Germany) according to the manufacturer's protocol. Gene expression was quantified by real-time quantitative PCR using SYBR Green PCR Master Mix (Applied Biosystems, Foster City, CA) and primers recognizing the viral *E1A* gene. DNA amplification was carried out using an Opticon 2 system (Bio-Rad, Foster City, CA), and the detection was performed by measuring the binding of the fluorescent dye,

SYBR green. Each sample was run in triplicates. Results are presented as the average number of *E1A* copies per ng of DNA (*E1A* copies per ng DNA).

We used the Adeno-X Rapid Titer Kit (Clontech, Mountain View, CA) according to the manufacturer's protocol to titrate the levels of infectious viral progeny. Briefly, infectious progeny were released from the infected cells by collecting infected cells and media from each group and subsequently subjecting them to three cycles of freezing and thawing. Cell lysates were then incubated with adherent HEK293 cells in serial tenfold dilutions. Forty-eight hours later, the amount of I.U. was calculated using the Adeno-X Rapid Titer Kit according to vendor recommendations. The titration units (I.U.) used by this protocol is similar to plaque-forming units.

Evaluation of relative gene expression by qRT-PCR. Relative expression of mRNA transcripts by NSCs was evaluated for the human receptors VEGFR2, CXCR4, and c-MET in addition to the cytokines IL-10, IL-6, interferon-γ, and TNF-α. Total cellular RNA was isolated using an RNeasy kit (Qiagen, Valencia, CA) according to the manufacturer's protocol and in each instance 1 µg of purified mRNA was reverse transcribed to complementary DNA using the iScript cDNA conversion kit (Bio-Rad). Quantitative PCR was conducted using the SYBR Green quantitative PCR kit (Invitrogen, Carlsbad, CA) for all experiments. Optimization of annealing temperatures for each transcript was first conducted. Each transcript of interest was amplified in triplicate at its proper annealing temperature and products were analyzed using the Opticon 2 software (Bio Rad, Hercules, CA). Amplification of the correct product was verified by running samples on 2% agarose gel electrophoresis and confirming product size. Relative expression was evaluated using the ΔC_T method ($\Delta C_T = C_T$ gene of interest $- C_T$ GAPDH) where a ΔC_T of 3.33 is equivalent to one magnitude change in gene expression. This logarithmic dependence was verified for each gene studied by conducting quantitative PCRs on a serial complementary DNA dilutions. Expression data are presented as fold change of the linearized ΔC_T ($2^{-\Delta CT}$) over control expression levels.

***Evaluation of NSC migration and viral delivery* in vitro.** To analyze the migratory and oncolytic adenovirus delivery characteristics of NSC *in vitro*, we used a similar system described earlier,[9] with a slight modification. To characterize the specificity of stem cell carrier migration in response to glioma, we used a BD Biocoat Tumor Invasion System (BD Biosciences, http://www.bdbiosciences.com) containing BD Falcon Fluoroblock 24-Multiwell inserts (8-µm pore size; PET membrane) in accordance with the manufacturer's protocol. To aid in the quantification of stem cell migration, fluorescently labeled NSCs (described above) were used. The migration was characterized with respect to four different types of conditioned media and a negative control. Conditioned media was obtained by culturing 1×10^5 cells of each cell type in serum-free/growth factor-free media for 24 hours, after which, equal amounts of each conditioned medium was aliquoted in the bottom wells of the migration chamber to act as a chemoattractant. For migration studies without adenovirus, NSCs were plated in serum-free minimum essential medium at a density of 5×10^4 cells/well. Twenty-four hours after plating NSCs into the top insert, the number of migrating cells/field view was counted using an Olympus IX81 inverted microscope and MetaMorph software (Olympus, Tokyo, Japan). Cells were counted in three random fields of view/well (original objective: 10×). A total of four wells was used for each experimental condition (i.e., U118MG = 4 wells).

For antibody-mediated blocking of tumor-tropic migration of NSCs, cells were infected with adenovirus for 16 hours, then cells were incubated with function-inhibiting antibody for CXCR4 (0.1 µg/µl), VEGFR2 (0.01 µg/µl), or the appropriate isotype control (R & D System, Minneapolis, MN) for 1 hour. These cells were then used in the migration assay as described above.

For studies involving NSC-mediated delivery of adenovirus, the same migration apparatus was used; however, NSCs were loaded with different I.U. of CRAd-S-pk7 virus before plating them in the top chamber of the migration apparatus (5×10^4 cells/well). Instead of conditioned medium, U87MG cells were plated in the bottom wells of the migration chamber in serum-free minimum essential medium at a density of 5×10^4 cells/well 2 days before plating stem cells in the top well of the migration chamber. The number of migrating cells was assessed as described above. Nonloaded NSCs were plated in chambers immersed in serum-free minimum essential medium as a reference control. Nine days after plating loaded NSCs in the top inserts, we quantified the number of I.U. in each of the bottom wells (4 wells/experimental condition) using the Adeno-X Rapid Titer kit as described above. Cytotoxicity resulting from stem cell release of viral progeny was quantified by counting the number U87MG glioma by trypan blue exclusion methods. Three random field views per well were captured; there were a total of 4 wells per experimental condition.

Flow cytometry. Flow cytometry of cell-surface antigens was performed as described.[9] The following antibodies were used: PE-conjugated anti-CD45 IgG, FITC-conjugated anti-CD11b (eBioscience, San Diego, CA), and rabbit polyclonal anti-GFAP (Abcam, Cambridge, MA). Data were acquired and analyzed in Canto with CellQuest (Becton Dickinson) and FlowJo (TreeStar, Ashland, OR) software. IL-10 enzyme-linked immunosorbent assay was performed by using an ELISE kit from eBioscience according to manufacturing protocol.

Animal studies. Intracranial glioma xenograft implantation: U87MG glioma cells were implanted *via* cranial guide screws as described previously. Briefly, mice were anesthetized with a ketamine/xylazine mixture (115/17 mg/kg), and a burr hole was made. Stereotactic injection was carried out by using a 10 µl Hamilton syringe (Hamilton, Reno, NV) with a 30-gauge needle, which was inserted through the burr hole to a depth of 3 mm mounted on a just for mice stereotactic apparatus (Harvard Apparatus, Holliston, MA). Male athymic/nude mice were obtained from Charles River Laboratory (Wilmington, MA). Animals were cared for according to a study-specific animal protocol approved by the University of Chicago Institutional Animal Care and Use Committee. To examine the virus progeny produced by NSCs, mice were injected with 2.5×10^5 U87MG cells in 5 µl/mouse. One week later, mice were randomly divided into six groups ($n = 3$ mice/group): one group received an injection of 5×10^5 NSC in 5 µl PBS/mouse (NSC) loaded with 50 I.U./NSC; one group received injections of 2.5×10^7 I.U. CRAd-S-pk7 in 5 µl/mouse (CRAd-S-pk7). Three mice from each group were killed and their brains were harvested. Single-cell suspensions were generated from each brain by homogenizing brain tissue in PBS (mg/ml). A 200 µl of homogenized tissue was further used to determine the progeny titer by using Adeno-X Rapid Titer kit as described above. For monitoring the GFAP-positive cells in the adenovirus-injected animal brains, we stereotactically injected an equivalent dose of CRAd-S-pk7 virus alone or loaded into NSCs as in the previous experiment into the animal brain. At the indicated time postinjection, three animals from each group were killed and single-cell suspension was generated as described above. GFAP-positive cells from each tissue were analyzed by fluorescence-activated cell sorting.

To evaluate the therapeutic efficacy of NSCs loaded with CRAd-S-pk7 virus, groups of nine nude mice were implanted with U87MG cells (2.5×10^5 cells in 5 µl PBS/mouse into the right hemisphere as previously described). Five days after tumor implantation, mice received an intracranial, intratumoral injection of 5×10^5 NSCs loaded with different doses of CRAd-S-pk7 virus or an equal dose of naked virus. Animals losing ≥30% of their body weight or having trouble ambulating, feeding, or grooming were killed by CO_2 intoxication followed by cervical dislocation. Brains underwent serial coronal sectioning (6 µm/section) for a total of 20–25 slices per tissue, altogether spanning ~3 mm of brain tissue. Representative hematoxylin–eosin-stained murine brain tissue pictures were captured using an AxioCam Color MR digital camera (http://www.zeiss.com/) attached to an Olympus BX41 microscope (original objective:

1.25×; http://www.olympus-global.com/en/global/) using AxioVision software, v. 3.0.

In vivo *photonflux image.* Mice were imaged for Fluc activity following intraperitoneal injection of D-luciferin (4.5 mg/animal in 150 µl saline), and photon counts were recorded 10 minutes after D-luciferin administration by using a cryogenically cooled high-efficiency charged-coupled device camera system (Xenogene).

Statistical analysis. The statistical analysis presented was performed using GraphPad Prism Software, v4.0 (GraphPad Software, La Jolla, CA). Where applicable, a standard independent two-sample *t*-test was applied. A P value <0.05 was considered statistically significant (***P value <0.001; **P value <0.01; *P value <0.05).

SUPPLEMENTARY MATERIAL

Figure S1. Comparative analysis of oncolytic virus replication in a permissive cell line A549 and the NSCs.

Figure S2. Analysis of bone marrow-derived macrophages in vivo.

Figure S3. Oncolytic virus loading into NSCs augments tumor-tropic migration *in vitro*.

ACKNOWLEDGMENTS

We thank Simona M. Ahmed for editing the manuscript and Dingcai Cao for statistical analysis. This research was supported by the NCI (R01CA122930, R01CA138587), the National Institute of Neurological Disorders and Stroke (U01NS069997), the American Cancer Society (RSG-07-276-01-MGO), and University of Chicago BSD IRI Pilot grants.

REFERENCES

1. Deorah, S, Lynch, CF, Sibenaller, ZA and Ryken, TC (2006). Trends in brain cancer incidence and survival in the United States: Surveillance, Epidemiology, and End Results Program, 1973 to 2001. *Neurosurg Focus* **20**: E1.
2. Dey, M, Ulasov, IV and Lesniak, MS (2010). Virotherapy against malignant glioma stem cells. *Cancer Lett* **289**: 1–10.
3. Fisher, K (2006). Striking out at disseminated metastases: the systemic delivery of oncolytic viruses. *Curr Opin Mol Ther* **8**: 301–313.
4. Aboody, KS, Brown, A, Rainov, NG, Bower, KA, Liu, S, Yang, W *et al.* (2000). Neural stem cells display extensive tropism for pathology in adult brain: evidence from intracranial gliomas. *Proc Natl Acad Sci USA* **97**: 12846–12851.
5. Benedetti, S, Pirola, B, Pollo, B, Magrassi, L, Bruzzone, MG, Rigamonti, D *et al.* (2000). Gene therapy of experimental brain tumors using neural progenitor cells. *Nat Med* **6**: 447–450.
6. Danks, MK, Yoon, KJ, Bush, RA, Remack, JS, Wierdl, M, Tsurkan, L *et al.* (2007). Tumor-targeted enzyme/prodrug therapy mediates long-term disease-free survival of mice bearing disseminated neuroblastoma. *Cancer Res* **67**: 22–25.
7. Sims, TL Jr, Hamner, JB, Bush, RA, Fischer, PE, Kim, SU, Aboody, KS *et al.* (2009). Neural progenitor cell-mediated delivery of osteoprotegerin limits disease progression in a preclinical model of neuroblastoma bone metastasis. *J Pediatr Surg* **44**: 204–210; discussion 210.
8. Coukos, G, Makrigiannakis, A, Kang, EH, Caparelli, D, Benjamin, I, Kaiser, LR *et al.* (1999). Use of carrier cells to deliver a replication-selective herpes simplex virus-1 mutant for the intraperitoneal therapy of epithelial ovarian cancer. *Clin Cancer Res* **5**: 1523–1537.
9. Tyler, MA, Ulasov, IV, Sonabend, AM, Nandi, S, Han, Y, Marler, S *et al.* (2009). Neural stem cells target intracranial glioma to deliver an oncolytic adenovirus *in vivo*. *Gene Ther* **16**: 262–278.
10. Willmon, C, Harrington, K, Kottke, T, Prestwich, R, Melcher, A and Vile, R (2009). Cell carriers for oncolytic viruses: Fed Ex for cancer therapy. *Mol Ther* **17**: 1667–1676.
11. Aboody, KS, Najbauer, J and Danks, MK (2008). Stem and progenitor cell-mediated tumor selective gene therapy. *Gene Ther* **15**: 739–752.
12. Einstein, O and Ben-Hur, T (2008). The changing face of neural stem cell therapy in neurologic diseases. *Arch Neurol* **65**: 452–456.
13. Pluchino, S, Quattrini, A, Brambilla, E, Gritti, A, Salani, G, Dina, G *et al.* (2003). Injection of adult neurospheres induces recovery in a chronic model of multiple sclerosis. *Nature* **422**: 688–694.
14. Pluchino, S, Zanotti, L, Rossi, B, Brambilla, E, Ottoboni, L, Salani, G *et al.* (2005). Neurosphere-derived multipotent precursors promote neuroprotection by an immunomodulatory mechanism. *Nature* **436**: 266–271.
15. Thomas, CE, Abordo-Adesida, E, Maleniak, TC, Stone, D, Gerdes, CA and Lowenstein, PR (2001). Gene transfer into rat brain using adenoviral vectors. *Curr Protoc Neurosci* **Chapter 4**: Unit 4.24.
16. Muruve, DA (2004). The innate immune response to adenovirus vectors. *Hum Gene Ther* **15**: 1157–1166.
17. Ulasov, IV, Zhu, ZB, Tyler, MA, Han, Y, Rivera, AA, Khramtsov, A *et al.* (2007). Survivin-driven and fiber-modified oncolytic adenovirus exhibits potent antitumor activity in established intracranial glioma. *Hum Gene Ther* **18**: 589–602.
18. Aghi, MK and Chiocca, EA (2009). Phase ib trial of oncolytic herpes virus G207 shows safety of multiple injections and documents viral replication. *Mol Ther* **17**: 8–9.
19. Haseley, A, Alvarez-Breckenridge, C, Chaudhury, AR and Kaur, B (2009). Advances in oncolytic virus therapy for glioma. *Recent Pat CNS Drug Discov* **4**: 1–13.
20. Ferguson, SD, Ahmed, AU, Thaci, B, Mercer, RW and Lesniak, MS (2010). Crossing the boundaries: stem cells and gene therapy. *Discov Med* **9**: 192–196.
21. Sun, L, Lee, J and Fine, HA (2004). Neuronally expressed stem cell factor induces neural stem cell migration to areas of brain injury. *J Clin Invest* **113**: 1364–1374.
22. Carbajal, KS, Schaumburg, C, Strieter, R, Kane, J and Lane, TE (2010). Migration of engrafted neural stem cells is mediated by CXCL12 signaling through CXCR4 in a viral model of multiple sclerosis. *Proc Natl Acad Sci USA* **107**: 11068–11073.
23. Heese, O, Disko, A, Zirkel, D, Westphal, M and Lamszus, K (2005). Neural stem cell migration toward gliomas *in vitro*. *Neuro-oncology* **7**: 476–484.
24. Schmidt, NO, Koeder, D, Messing, M, Mueller, FJ, Aboody, KS, Kim, SU *et al.* (2009). Vascular endothelial growth factor-stimulated cerebral microvascular endothelial cells mediate the recruitment of neural stem cells to the neurovascular niche. *Brain Res* **1268**: 24–37.
25. Magge, SN, Malik, SZ, Royo, NC, Chen, HI, Yu, L, Snyder, EY *et al.* (2009). Role of monocyte chemoattractant protein-1 (MCP-1/CCL2) in migration of neural progenitor cells toward glial tumors. *J Neurosci Res* **87**: 1547–1555.
26. Ramalingam, R, Worgall, S, Rafii, S and Crystal, RG (2000). Downregulation of CXCR4 gene expression in primary human endothelial cells following infection with $E1^{-}E4^{+}$ adenovirus gene transfer vectors. *Mol Ther* **2**: 381–386.
27. Ulasov, IV, Tyler, MA, Han, Y, Glasgow, JN and Lesniak, MS (2007). Novel recombinant adenoviral vector that targets the interleukin-13 receptor α2 chain permits effective gene transfer to malignant glioma. *Hum Gene Ther* **18**: 118–129.
28. de la Monte SM, Ho DD, Schooley RT, Hirsch MS and Richardson EP Jr. (1987). Subacute encephalomyelitis of AIDS and its relation to HTLV-III infection. *Neurology* **37**: 562–569.
29. Brodie, C, Weizman, N, Katzoff, A, Lustig, S and Kobiler, D (1997). Astrocyte activation by Sindbis virus: expression of GFAP, cytokines, and adhesion molecules. *Glia* **19**: 275–285.
30. Montgomery, DL (1994). Astrocytes: form, functions, and roles in disease. *Vet Pathol* **31**: 145–167.
31. Woiciechowsky, C, Schöning, B, Stoltenburg-Didinger, G, Stockhammer, F and Volk, HD (2004). Brain-IL-1 beta triggers astrogliosis through induction of IL-6: inhibition by propranolol and IL-10. *Med Sci Monit* **10**: BR325–BR330.
32. Ulasov, IV, Tyler, MA, Rivera, AA, Nettlebeck, DM, Douglas, JT and Lesniak, MS (2008). Evaluation of E1A double mutant oncolytic adenovectors in anti-glioma gene therapy. *J Med Virol* **80**: 1595–1603.